articles

molecular pharmaceutics

Cationic Poly-L-lysine Dendrimers: Pharmacokinetics, Biodistribution, and Evidence for Metabolism and Bioresorption after Intravenous Administration to Rats

Ben J. Boyd,[†] Lisa M. Kaminskas,[†] Peter Karellas,[†,‡] Guy Krippner,[‡] Romina Lessene,[‡] and Christopher J. H. Porter*[,†]

Department of Pharmaceutics, Victorian College of Pharmacy, Monash University, 381 Royal Parade, Parkville, VIC, 3052, Australia, and Starpharma Pty. Ltd., Level 6, Baker Heart Research Building, Commercial Road, Melbourne, VIC, 3004, Australia

Received March 15, 2006

Abstract: Cationic poly-L-lysine ^{3}H-dendrimers with either 16 or 32 surface amine groups (BHALys $[Lys]_4$ $[^3H\text{-}Lys]_8$ $[NH_2]_{16}$ and BHALys $[Lys]_8$ $[^3H\text{-}Lys]_{16}$ $[NH_2]_{32}$, generation 3 and 4, respectively) have been synthesized and their pharmacokinetics and biodistribution investigated after intravenous administration to rats. The species in plasma with which radiolabel was associated was also investigated by size exclusion chromatography (SEC). Rapid initial removal of radiolabel from plasma was evident for both dendrimers ($t_{1/2}$ < 5 min). Approximately 1 h postdose, however, radiolabel reappeared in plasma in the form of free lysine and larger (but nondendrimer) species that coeluted with albumin by SEC. Plasma and whole blood pharmacokinetics were similar, precluding interaction with blood components as a causative factor in either the rapid removal or reappearance of radioactivity in plasma. Administration of monomeric ^{3}H L-lysine also resulted in the appearance in plasma of a radiolabeled macromolecular species that coeluted with albumin by SEC, suggesting that biodegradation of the dendrimer to L-lysine and subsequent bioresorption may explain the pharmacokinetic profiles. Capping the Lys_8 dendrimer with D-lysine to form BHALys $[Lys]_4$ $[^3H\text{-}Lys]_8$ $[D\text{-}Lys]_{16}$ $[NH_2]_{32}$ resulted in similar, and very rapid, initial disappearance kinetics from plasma when compared to the L-lysine capped dendrimer. Since significant extravasation of these large hydrophilic molecules seems unlikely, this most likely reflects both elimination and extensive binding to vascular surfaces. Capping with "non-natural" D-lysine also appeared to render the dendrimer essentially inert to the biodegradation process. For the L-lysine capped dendrimers, radiolabel was widely distributed throughout the major organs, with no apparent selectivity for organs of the reticuloendothelial system. In contrast, a greater proportion of the administered radiolabel was recovered in the organs of the reticuloendothelial system for the D-lysine capped system, as might be expected for a nondegrading circulating foreign colloid. To our knowledge this is the first data to demonstrate the biodegradation/bioresorption of poly-L-lysine dendrimers and has significant implications for the utility of these systems as drugs or drug delivery systems.

Keywords: Dendrimer; pharmacokinetics; poly-L-lysine; biodegradation; biodistribution

Introduction

Dendrimers are macromolecules prepared by a stepwise synthetic approach that adds multivalent "layers" to a core structure. The physical size of dendrimers (usually described by a hydrodynamic diameter) may vary widely (1−100 nm) but is typically regarded as being between that of a small molecule and that of a colloidal particle. As such dendritic macromolecules share properties in common with both typical small molecules and larger colloidal species. They have a polymeric structure and, when constructed from amino acids, may also have the functionality of proteins. The molecular versatility of dendrimers is almost infinite, and the structure of the core and additional multivalent mono-

* Corresponding author. Mailing address: Department of Pharmaceutics, Victorian College of Pharmacy, Monash University, 381 Royal Pde, Parkville, VIC, 3052, Australia. Phone: +61399039649. Fax: +61399039583. E-mail: Chris.porter@vcp.monash.edu.au.

† Monash University.

‡ Starpharma Pty. Ltd.

10.1021/mp060032e CCC: $33.50
Published on Web 08/04/2006

mers, the number of layers, and the terminal surface groups can all be altered.[1] This provides for variation in size, molecular weight, surface charge, symmetry of molecular shape, and hydrophilicity, all of which may impact on chemical and pharmacological properties. Consequently a number of potential uses across various technological fields are becoming evident.[2] In the pharmaceutical field there has been significant interest in the use of dendrimers as carriers for therapeutic compounds, either by covalently linking drug molecules to the dendrimer surface or by drug solubilization within a hydrophobic core or pocket within the dendrimer.[3−11] Covalent attachment of drug molecules to the surface of dendrimers has also shown potential from a stability and targeting perspective, particularly in the anticancer field.[12−15] Importantly, dendrimers are also receiving attention as therapeutic entities in their own right, with SPL7013 Gel (VivaGel) being the first dendrimer-based therapeutic compound currently in clinical trials under an Investigational New Drug Application (IND) with the U.S. Food and Drug Administration (FDA).

The interaction of dendrimers with intestinal tissues has been the subject of several studies,[16−23] and while trends in permeability and cytotoxicity with surface charge and surface functionality have been established, relatively few studies have described the fate of dendrimers once absorbed into the systemic circulation. Of these few studies, Gillies et al.[24] have examined the pharmacokinetics of PEGylated, "bow-tie" polyester dendrimers and shown that dendrimer clearance mechanisms are highly dependent on the molecular weight and flexibility of the complex. Also, several investigators have examined the effect of structural changes on the biodistribution of dendrimers designed to facilitate heavy metal or antibody complexation (and therefore application in bioimaging).[25−29] To this point, however, the intrinsic systemic pharmacokinetics of polylysine dendrimers have not been described in any detail, and in particular the effects of size and surface functionality on clearance, distribution,

(1) Zeng, F. W.; Zimmerman, S. C. Dendrimers in Supramolecular Chemistry: From Molecular Recognition to Self-Assembly. *Chem. Rev.* **1997**, *97*, 1681−1712.

(2) Frechet, J. M. J. Dendrimers and Other Dendritic Macromolecules: From Building Blocks to Functional Assemblies in Nanoscience and Nanotechnology. *J. Polym. Sci. A* **2003**, *41*, 3713−3725.

(3) Aulenta, F.; Hayes, W.; Rannard, S. Dendrimers: A New Class of Nanoscopic Containers and Delivery Devices. *Eur. Polym. J.* **2003**, *39*, 1741−1771.

(4) Liu, M. J.; Frechet, J. M. J. Designing Dendrimers for Drug Delivery. *Pharm. Sci. Technol. Today* **1999**, *2*, 393−401.

(5) Jansen, J. F. G. A.; de Brabander-van den Berg, E. M. M.; Meijer, E. W. Encapsulation of Guest Molecules into a Dendritic Box. *Science* **1994**, *266*, 1226−1229.

(6) Liu, M. J.; Kono, K.; Frechet, J. M. J. Water-Soluble Dendritic Unimolecular Micelles: Their Potential as Drug Delivery Agents. *J. Controlled Release* **2000**, *65*, 121−131.

(7) Milhem, O. M.; Myles, C.; McKeown, N. B.; Attwood, D.; D'Emanuele, A. Polyamidoamine Starburst Dendrimers as Solubility Enhancers. *Int. J. Pharm.* **2000**, *197*, 239−241.

(8) Beezer, A. E.; King, A. S. H.; Martin, I. K.; Mitchel, J. C.; Twyman, L. J.; Wain, C. F. Dendrimers as Potential Drug Carriers; Encapsulation of Acidic Hydrophobes Within Water Soluble PAMAM Derivatives. *Tetrahedron* **2003**, *59*, 3873−3880.

(9) Baars, M. W. P. L.; Meijer, E. W. Host−Guest Chemistry of Dendritic Molecules. *Top. Curr. Chem.* **2000**, *210*, 131−182.

(10) Pistolis, G.; Malliaris, A.; Paleos, C. M.; Tsiourvas, D. Study of Poly(Amidoamine) Starburst Dendrimers by Fluorescence Probing. *Langmuir* **1997**, *13*, 5870−5875.

(11) Kojima, C.; Kono, K.; Maruyama, K.; Takagishi, T. Synthesis of Polyamidoamine Dendrimers Having Poly(ethylene glycol) Grafts and Their Ability To Encapsulate Anticancer Drugs. *Bioconjugate Chem.* **2000**, *11*, 910−917.

(12) Ihre, H. R.; Padilla De Jesus, O. L.; Szoka, F. C. Jr.; Frechet, J. M. J. Polyester Dendritic Systems For Drug Delivery Applications: Design, Synthesis, and Characterization. *Bioconjugate Chem.* **2002**, *13*, 443−452.

(13) Quintana, A.; Raczka, E.; Piehler, L.; Lee, I.; Myc, A.; Majoros, I.; Patri, A. K.; Thomas, T.; Mule, J.; Baker, J. R. Design and Function of a Dendrimer-Based Therapeutic Nanodevice Targeted to Tumor Cells Through the Folate Receptor. *Pharm. Res.* **2002**, *19*, 1310−1316.

(14) Jelinkova, M.; Strohalm, J.; Etrych, T.; Ulbrich, K.; Rihova, B. Starlike vs. Classic Macromolecular Prodrugs: Two Different Antibody-Targeted HPMA Copolymers of Doxorubicin Studied In Vitro and In Vivo as Potential Anticancer Drugs. *Pharm. Res.* **2003**, *20*, 1558−1564.

(15) Malik, N.; Evagorou, E. G.; Duncan, R. Dendrimer-Platinate: A Novel Approach to Cancer Chemotherapy. *Anti-Cancer Drugs* **1999**, *10*, 767−776.

(16) Tajarobi, F.; El-Sayed, M.; Rege, B. D.; Polli, J. E.; Ghandehari, H. Transport of Poly Amidoamine Dendrimers Across Madin-Darby Canine Kidney Cells. *Int. J. Pharm.* **2001**, *215*, 263−267.

(17) El-Sayed, M.; Ginski, M.; Rhodes, C.; Ghandehari, H. Transepithelial Transport of Poly(Amidoamine) Dendrimers Across Caco-2 Cell Monolayers. *J. Controlled Release* **2002**, *81*, 355−365.

(18) Malik, N.; Wiwattanapatapee, R.; Klopsch, R.; Lorenz, K.; Frey, H.; Weener, J. W.; Meijer, E. W.; Paulus, W.; Duncan, R. Dendrimers: Relationship Between Structure and Biocompatibility In Vitro, and Preliminary Studies on the Biodistribution of I-125-Labelled Polyamidoamine Dendrimers In Vivo. *J. Controlled Release* **2000**, *65*, 133−148.

(19) Wiwattanapatapee, R.; Carreno-Gomez, B.; Malik, N.; Duncan, R. Anionic PAMAM Dendrimers Rapidly Cross Adult Rat Intestine In Vitro: A Potential Oral Delivery System? *Pharm. Res.* **2000**, *17*, 991−998.

(20) Jevprasesphant, R.; Penny, J.; Jalal, R.; Attwood, D.; McKeown, N. B.; D'Emanuele, A. The Influence of Surface Modification on the Cytotoxicity of PAMAM Dendrimers. *Int. J. Pharm.* **2003**, *252*, 263−266.

(21) Sakthivel, T.; Toth, I.; Florence, A. T. Distribution of a Lipidic 2.5 nm Diameter Dendrimer Carrier After Oral Administration. *Int. J. Pharm.* **1999**, *183*, 51−55.

(22) Florence, A. T.; Sakthivel, T.; Toth, I. Oral Uptake and Translocation of a Polylysine Dendrimer with a Lipid Surface. *J. Controlled Release* **2000**, *65*, 253−259.

(23) Jevprasesphant, R.; Penny, J.; Attwood, D.; D'Emanuele, A. Transport of Dendrimer Nanocarriers Through Epithelial Cells via the Transcellular Route. *J. Controlled Release* **2004**, *97*, 259−267.

(24) Gillies, E. R.; Dy, E.; Fréchet, J. M. J.; Szoka, F. C. Biological Evaluation of Polyester Dendrimer: Poly(ethylene oxide) "Bow-Tie" Hybrids with Tunable Molecular Weight and Architecture. *Mol. Pharm.* **2005**, *2*, 129−138.

Scheme 1. Scheme Depicting the Synthesis of a Generation 4 Poly-lysine Dendrimer with 16 Surface Lysine Groups[a]

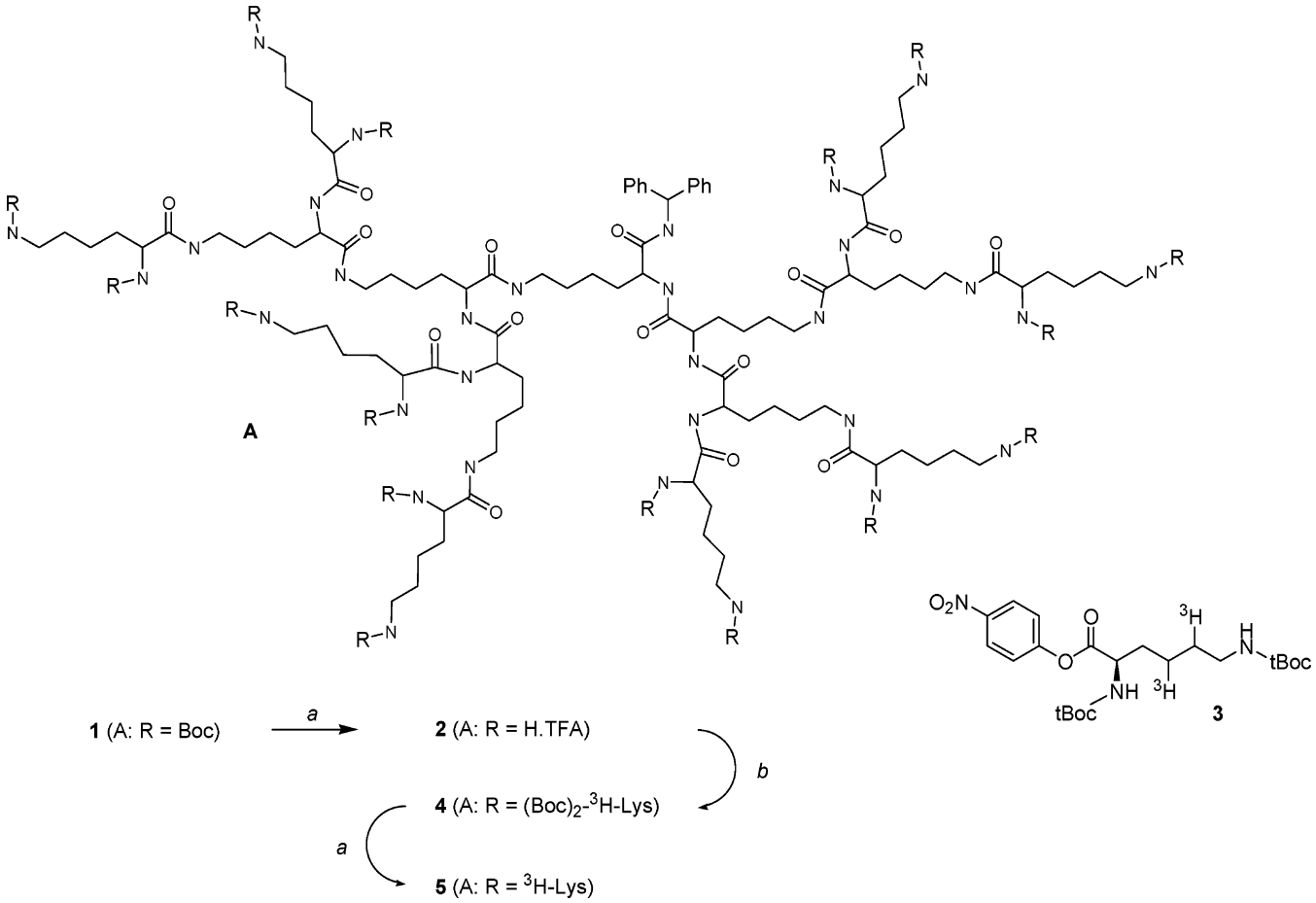

[a] Structure **A** is a general structure representing a generation 3 poly-L-lysine dendrimer with R groups attached to the primary amines on the terminal lysine. Structure **A** where R = Boc is the Boc-protected generation 3 poly-L-lysine dendrimer (**1**); this is deprotected (reaction a) to form the generation 3 poly-L-lysine dendrimer, which may be isolated as the TFA salt (**2**, structure **A** where R = H). A subsequent layer of ^{3}H-labeled and Boc-protected lysine (**3**) is then added (reaction b) to form the labeled, protected generation 4 dendrimer (**4**), which is in turn deprotected to provide the final ^{3}H-labeled, generation 4 poly-L-lysine dendrimer (**5**, structure **A** where R = ^{3}H-lysine). The ^{3}H-labeled generation 3 dendrimer is synthesized in an analogous fashion, but starting with the generation 2 unlabeled material.

and metabolism patterns (and potential bioresorption) have yet to be reported.

As such, the current study is the first in a series of reports aimed at determining the influence of dendrimer size (molecular weight or generation), surface charge, and surface functionality on the pharmacokinetics and biodistribution of poly-L-lysine based dendrimers after intravenous administration. In the current study, ^{3}H-labeled poly-L-lysine dendrimers (Scheme 1, Table 1), with either third (BHALys $[Lys]_4$ $[^3H\text{-}Lys]_8$ $[NH_2]_{16}$) or fourth (BHALys $[Lys]_8$ $[^3H\text{-}Lys]_{16}$ $[NH_2]_{32}$) generation cores, have been prepared and the surfaces left uncapped as L-lysine. By way of comparison, a third dendrimer consisting of the Lys_8 core capped with D-lysine, essentially forming a Lys_{16} dendrimer with D-lysine at its

(25) Kobayashi, H.; Kawamoto, S.; Saga, T.; Sato, N.; Hiraga, A.; Konishi, J.; Togashi, K.; Brechbiel, M. W. Micro-MR Angiography of Normal and Intratumoral Vessels in Mice Using Dedicated Intravascular MR Contrast Agents with High Generation of Polyamidoamine Dendrimer Core: Reference to Pharmacokinetic Properties of Dendrimer-Based MR Contrast Agents. *J. Magn. Reson. Imaging* **2001**, *14*, 705−713.

(26) Kobayashi, H.; Wu, C. C.; Kim, M. K.; Paik, C. H.; Carrasquillo, J. A.; Brechbiel, M. W. Evaluation of the In Vivo Biodistribution of Indium-111 and Yttrium-88 Labeled Dendrimer-1B4M-DTPA and its Conjugation with Anti-Tac Monoclonal Antibody. *Bioconjugate Chem.* **1999**, *10*, 103−111.

(27) Kobayashi, H.; Saga, T.; Kawamoto, S.; Sato, N.; Hiraga, A.; Ishimori, T.; Konishi, J.; Togashi, K.; Brechbiel, M. W. Dynamic Micro-Magnetic Resonance Imaging of Liver Micrometastasis in Mice with a Novel Liver Macromolecular Magnetic Resonance Contrast Agent DAB-Am64-(1B4M-Gd)(64). *Cancer Res.* **2001**, *61*, 4966−4970.

(28) Kobayashi, H.; Kawamoto, S.; Saga, T.; Sato, N.; Hiraga, A.; Ishimori, T.; Konishi, J.; Togashi, K.; Brechbiel, M. W. Positive Effects of Polyethylene Glycol Conjugation to Generation-4 Polyamidoamine Dendrimers as Macromolecular MR Contrast Agents. *Magn. Reson. Med.* **2001**, *46*, 781−788.

(29) Margerum, L. D., Campion, B. K.; Koo, M.; Shargill, N.; Lai, J. J.; Marumoto, A.; Sontum, P. C. Gadolinium(III) DO3A Macrocycles and Polyethylene Glycol Coupled to Dendrimers—Effect of Molecular Weight on Physical and Biological Properties of Macromolecular Magnetic Resonance Imaging Contrast Agents. *J. Alloys Compd* **1997**, *249*, 185−190.

Table 1. Selected Properties of the Dendrimers Used in This Study[a]

dendrimer	no. of free amines on the surface	molecular mass (Da)	specific activity (μCi/mg, mean ± SD, $n = 3$)
BHALys $[Lys]_4$ $[^3H\text{-}Lys]_8$ $[NH_2]_{16}$	16	2106	0.531 ± 0.012
BHALys $[Lys]_8$ $[^3H\text{-}Lys]_{16}$ $[NH_2]_{32}$	32	4158	0.422 ± 0.012
BHALys $[Lys]_4$ $[^3H\text{-}Lys]_8$ $[D\text{-}Lys]_{16}$ $[NH_2]_{32}$	32	4157	4.186 ± 0.087

[a] The number of free amines present on the surface of the dendrimers is given in the table. These values represent the number of "uncapped" amines on the outer layer of each dendrimer which was confirmed by mass spectra that indicated that the major ions were those of the fully deprotected dendrimers. The molecular masses listed for each dendrimer were determined by LC/MS, and the MS spectra (and theoretical masses) for each dendrimer are given in the Supporting Information.

outer layer (BHALys $[Lys]_4$ $[^3H\text{-}Lys]_8$ $[D\text{-}Lys]_{16}$ $[NH_2]_{32}$), has also been examined. In all cases, the dendrimers were covered with cationic amine groups at physiological pH. The in vivo fate of the ^3H dendrimers was further studied by separation of the different radiolabeled species present in plasma using size exclusion chromatography. The data suggest that poly-L-lysine dendrimers are rapidly removed from plasma after intravenous administration, but they are subsequently metabolized and the liberated L-lysine is reincorporated into endogenous resynthetic processes.

Method

Materials. Chemicals were purchased from Aldrich and used without further purification. Unlabeled amino acids for synthesis were purchased from Bachem (Bunbendorf, Switzerland). All solvents were HPLC grade and used without further purification. (L)-(4,5-^{3}H)-Lysine (1 mCi/mL) was purchased from MP Biomedicals (Irvine, CA). Lysine dendrimer precursors were prepared according to published procedures.[30] Buffer (phosphate-buffered saline, PBS) reagents (KH_2PO_4, Na_2HPO_4, NaCl, KCl) were AR grade. Water was obtained from a MilliQ water purification system (Millipore, Australia). Heparin (10 000 IU/mL) was obtained from Faulding, Australia. Saline for injection was obtained in 100 mL polyethylene bags from Baxter Healthcare Pty. Ltd. (NSW, Australia). Nonradiolabeled L-lysine was obtained from Sigma Chemical Co. (St. Louis, MO). Starscint scintillation cocktail and Soluene-350 tissue solubilizer were purchased from Packard Biosciences (Meriden, CT). Protein standards included blue dextran 2000 (2000 kDa), fatty acid free bovine serum albumin (67 kDa), pepsin (35 kDa), trypsin (23.8 kDa), myoglobin (17.6 kDa), ribonuclease A (13.7 kDa), cytochrome C (12.4 kDa), and vitamin B12 (1.4 kDa) and were all obtained from Sigma Chemical Co. (St. Louis, MO).

Synthesis and Characterization of Tritium-Labeled Cationic Dendrimers. The lysine dendrimers were synthesized using the procedure originally developed by Denkewalter.[31] The tritium radiolabel was incorporated using a lysine moiety that contained tritium labels at the γ and δ positions (see Scheme 1), and this was most efficient (in terms of conserving specific activity) if used in the outermost layer of the dendrimer. The dendrimer nomenclature employed makes use of the following notation:

$$\text{core [last complete "unlabeled" layer]}_n\ [^3\text{H-labeled layer}]_m\ [\text{terminal group}]_p$$

where "core" is the molecule to which the activated lysine generation building units are attached (which in this article is the benzhydrylamide of lysine BHALys); "last complete unlabeled layer" consists of the nontritiated species making up the last layers of the dendrimer (L-Lys), and n is the number of these groups; "^{3}H-labeled layer" is the tritiated layer (^{3}H-Lys), and m is the number of these groups; and "terminal group" is the capping group (NH_2 in the case of the products and Boc in the case of the intermediates), and p is the number of these terminal groups. For the dendrimer containing a D-lysine layer, the ^{3}H-labeled layer is the last L-lysine layer before addition of D-lysine, and the nomenclature for this is

$$\text{core [last complete "unlabeled" layer]}_n\ [^3\text{H-labeled layer}]_m\ [\text{D-Lys layer}]_o\ [\text{terminal group}]_p$$

where o is the number of these groups (NH_2 in the case of the products and Boc in the case of the intermediates) and m is the number of these terminal groups.

This nomenclature is able to completely describe the structure of a dendrimer through provision of the core and the outer layer since only lysine building units are used in the construction of these macromolecule structures and the valency of the core is known; and further, since all of the surface amine groups of each macromolecule layer are completely reacted with lysine during the addition of a new lysine layer, it follows that, for an outer layer of 8 lysines, there is a subsurface layer of 4 lysines and a second subsurface layer of 2 lysines that are connected to the divalent BHALys core.

The preparation of lysine dendrimers from the benzhydryl amide protected lysine core has been described in detail elsewhere,[30] and detailed methods are given in the Supporting Information. The materials have been prepared in multi-100 g batches with a high degree of purity using iterative cycles of Boc deprotection and reaction of the TFA salts with excess of the *p*-nitrophenol active ester of α,ϵ-(*t*-Boc)$_2$-(L)-lysine as part of the scale-up manufacture of SPL7013, the active antiviral component in VivaGel, a topical microbicide gel

(30) Matthews, B. R.; Holan, G. Antiviral Dendrimers. 2001, U.S. Patent 6,190,650.

(31) Denkewalter, R. G.; Kolc, J. F.; Lukasavage, W. J. Preparation of Lysine Based Macromolecular Highly Branched Homogeneous Compound. 1979, U.S. Patent 4,360,646.

under development by Starpharma Pty. Ltd. The multi-Boc protected materials and the multi-TFA salts are both solids that can be further purified through washing and precipitation steps. The materials are readily analyzed using HPLC/(ESI)-MS, a technique that can resolve single deletion impurities and provide identity information (as molecular ions) for target materials as well as byproducts.

The tritium isotope was incorporated into the dendrimer by way of the *p*-nitrophenol active ester of α,ϵ-(*t*-Boc)$_2$-(L)−(4,5-^{3}H)-lysine. The dendrimeric precursor is the multi-Boc dendrimer one generation (or lysine layer) smaller. In a typical preparation BHALys [Lys]$_8$ [Boc]$_{16}$ was taken up in TFA and stirred for 4 h. The TFA was then removed under vacuum to give the desired TFA salt. This TFA salt in DMF with excess α,ϵ-(*t*-Boc)$_2$-(L)−(4,5-^{3}H)-lysine *p*-nitrophenol ester and triethylamine was allowed to react overnight. A yellow solid separated when the crude reaction was added to ice water. This crude product was washed with acetonitrile to purify. Analysis of this material by ^{1}H NMR and HPLC/(ESI)MS confirmed the identity and purity (>90%) of the BHALys [Lys]$_8$ [^{3}H-Lys]$_{16}$ [Boc]$_{32}$. The cationic dendrimer BHALys [Lys]$_8$ [^{3}H-Lys]$_{16}$ [NH$_2$]$_{32}$ was then provided by a similar Boc deprotection step using TFA. Purification prior to supply was via ultrafiltration or size exclusion chromatography (Sephadex LH20, eluted with water), and ion exchange (OH$^-$ form) to provide the free base form of the amine-terminated dendrimers as white lyophilates.

Purity was ascertained by HPLC, NMR, and mass spectrometry. NMR spectra were recorded in d_6-DMSO, D_2O, CD_3OD, or $CDCl_3$ on a Bruker (Bruker Daltronics Inc., NSW, Australia) 300 UltraShield 300 MHz NMR instrument. HPLC/(ESI)MS were conducted on a Waters (Millipore Corporation, Milford, MA) 2795 with 2996 diode array detector (DAD) coupled to a Waters ZQ4000 with ESI probe, inlet flow split to give approximately 50 μL/min to the MS. ^{3}H-L-Lysine (25 μCi) was freshly diluted with nonradiolabeled lysine in phosphate-buffered saline (PBS, pH 7.4) to a final specific activity of 20 μCi/mg for IV dosing. All dendrimers were diluted in PBS and frozen at −20 °C until used.

Activity Determinations and Scintillation Counting. The specific activity of the dendrimers was determined in triplicate by dilution of stock solutions containing known mass into PBS. An aliquot was subsequently added to 1 mL of Starscint and scintillation counted on a Packard Tri-Carb 2000CA liquid scintillation analyzer (Meriden, CT). The average of the triplicate determinations was used for all subsequent calculations.

Animals. Male Sprague Dawley rats (250−350 g) were used in these experiments. Rats were provided with water at all times and were maintained on a 12 h light/dark cycle in an ambient temperature of 21−22 °C. Food was withheld after surgery and until 8 h after administration of the iv dose. Food was provided at all other times. All animal experimentation protocols were approved by the Victorian College of Pharmacy Animal Ethics Committee, Monash University, Parkville, VIC, Australia.

Intravenous Pharmacokinetic Studies. Prior to dendrimer administration, rats had cannulas (polyethylene tubing 0.96 × 0.58 mm, Paton Scientific, Victor Harbour, Australia) inserted into the jugular vein and carotid artery, under isoflurane anesthesia as described previously.[32] The cannulas were flushed with heparinized saline (2 IU/mL) and flame sealed before insertion into a subcutaneous pocket at the back of the neck during recovery. The rats were allowed to recover overnight prior to dosing. Food was withheld for 12 h prior to dosing. After the recovery period rats were housed in metabolic cages to permit separate collection of urine and feces, and the cannulas were attached to a swivel/leash assembly to facilitate drug administration and blood collection. Free access to water was allowed at all times. L-Lysine or the dendrimers were dissolved in 1 mL of phosphate-buffered saline (PBS) and administered at a dose of 5 mg/kg by intravenous infusion over 2 min via the indwelling jugular cannula. The cannula was then flushed with 0.25 mL of heparinized saline to ensure complete infusion of the dose. Blood samples (0.15 mL) were subsequently obtained from the carotid artery at the following nominal time points: prior to dosing (−5 min), at the instant of conclusion of infusion ($t = 0$) and at 5, 10, 20, 30, 45, 60, 90, 120, 180, 240, 360, 480, 1440, and 1800 min. Blood samples were placed immediately into tubes containing 10 IU of heparin and centrifuged for 5 min at 3500*g*. Plasma (50 μL) was then added to 1 mL of Starscint scintillation cocktail and vortexed before scintillation counting. The limit of quantitation for the plasma assay (20 disintegrations per minute (dpm)) was validated using replicate ($n = 5$) analyses of spiked plasma samples and was defined as the lowest level of spiked activity that could be assayed with appropriate accuracy and precision (within ±20%).

Biodistribution Studies. In order to understand the fate of dendrimers in vivo, the biodistribution to various major organs was investigated. On completion of the pharmacokinetic studies (30 h), animals were sacrificed by injection of a lethal dose of sodium pentobarbital and the following tissues removed by dissection: heart, lungs, liver, spleen, pancreas, kidneys, and brain. The tissues were stored frozen (−20 °C) in preweighed polypropylene tubes until immediately prior to tissue treatment and analysis.

Tissues were initially treated by homogenizing the sample in a Waring miniblender (Extech Equipment Pty. Ltd., Boronia, Australia) with 5−10 mL of MilliQ water for 5 × 10 s intervals. In developing a method to measure the relatively low levels of radioactivity in the tissue samples, problems were encountered with chemiluminescence reactions and color quenching, leading to highly variable background counts on scintillation counting. These problems also appeared to be exacerbated by increases in temperature,

(32) Lyons, K. C.; Charman, W. N.; Miller, R.; Porter, C. J. Factors Limiting the Oral Bioavailability of N-Acetylglucosaminyl-N-Acetylmuramyl Dipeptide (GMDP) and Enhancement of Absorption in Rats by Delivery in a Water-in-Oil Microemulsion. *Int. J. Pharm.* **2000**, *199*, 17−28.

exposure to light, and agitation of the samples. In order to overcome these problems, the subsequent treatment of the tissues was conducted as a two stage process.

An initial "screening" stage was used to determine the approximate levels of radioactivity in the samples. For this stage a single sample from each tissue homogenate (typically 40−100 mg of tissue) was placed into a 20 mL polypropylene scintillation vial containing 2 mL of Soluene and tissue digestion allowed to occur at 60 °C overnight. 2-Propanol (2 mL) was then added and the solution heated for a further 2 h at 60 °C. On cooling to room temperature, 2 × 100 μL aliquots of hydrogen peroxide (30% w/v) were added sequentially to the samples, which were then allowed to stand at room temperature until bubbling had ceased. Starscint (12 mL) was then added and the mixture vortexed before the samples were stored at 4 °C for 96 h in the dark without agitation. The samples were then scintillation counted, during which time the counter was maintained at 12 °C using a cooled sample tray. Samples were also counted in sets of six to twelve to minimize warming during counting. Single samples were also taken from organs from untreated rats and processed in a similar manner to obtain a value for background counts expected due to the processing method alone. These values were subtracted from the values obtained during the screening stage. The data obtained from this screening stage provided a broad indication of the expected quantities of activity in each sample. This information was required for the subsequent "analytical" runs.

In the second "analytical" stage of the tissue counting process, tissue samples were analyzed in triplicate. Blank tissues from untreated rats were also processed as above (albeit in triplicate) to provide for background correction. Homogenized tissues from dendrimer-dosed rats were in general processed in a fashion identical to that described in the screening stage above, except that additional steps were taken to correct for any reduction in radioactivity counting efficacy (quench) due to the "extraction" process from the tissue. To allow correction for counting efficiency, an identical second set of tissues from treated rats was processed in the same way but was initially spiked with a known quantity of radiolabeled dendrimer prior to addition of Soluene. Tissues were spiked with activity at a level approximately equivalent to that measured in the screening samples (hence the need for the screening data). A processing efficiency was then calculated, where

$$\text{efficiency} = \frac{\text{spiked tissue}_{\text{dpm}} - \text{tissue}_{\text{dpm,uncorr}}}{\text{spiked soln}_{\text{dpm}}} \qquad (1)$$

Spiked $\text{tissue}_{\text{dpm}}$ was the mass-corrected radioactivity measured in the spiked samples, $\text{tissue}_{\text{dpm,uncorr}}$ was the mass-corrected radioactivity in the tissue samples which have not had an additional radioactivity spike added, and spiked soln_{dpm} was the known amount of additional radioactivity added to the spiked sample. Effectively, the calculation provides an indication of the efficiency of counting, using the known (spiked) amount of radioactivity in each tissue as a reference.

This value for efficiency was then used to correct the ^{3}H content in the processed sample where

$$\text{tissue}_{\text{dpm,corr}} = \frac{\text{tissue}_{\text{dpm, uncorr}}}{\text{efficiency}} \qquad (2)$$

The activity in the whole organ was then calculated knowing the mass fraction of the entire organ present in the processed sample. The results are expressed as either the percentage of injected dose in the organ at sacrifice or the percentage of injected dose per gram of tissue. Due to the variability of the process, an LOQ (limit of quantification) could not be easily determined for each tissue. Instead, triplicate samples resulting in a % CV greater than 20% either were repeated or were classified as below the quantifiable level when reproducible data could not be obtained.

Whole Blood Pharmacokinetics. To determine whole blood pharmacokinetics, separate groups of animals were administered identical quantities of the dendrimer solutions and whole blood samples (150 μL) collected into heparinized Eppendorf tubes at the same nominal time periods as that used for collection of plasma. Duplicate aliquots (50 μL) of each blood sample were added to 2 × 20 mL scintillation vials. Initially, one vial was untreated while the other was spiked with a known quantity (∼300−600 dpm of the dendrimer being investigated) to provide whole blood counting efficiency data (as above). The samples were then solubilized in 4 mL of a 1:1 ratio of Soluene-350 and isopropyl alcohol at 60 °C overnight. Samples were subsequently cooled and bleached with 200 μL of hydrogen peroxide (30% w/v) before the addition of Starscint (12 mL). Samples were then left at room temperature for 24 h prior to scintillation counting. The counts obtained from the blood samples were corrected for efficiency by comparison with the data obtained for the spiked sample as described above.

Urine and Feces. Urine from dendrimer dosed rats was collected over three time intervals: 0−8 h, 8−24 h, and 24−30 h postdosing. A blank urine sample obtained from each rat before dosing was also collected. A 100 μL aliquot of the urine from each time interval was added to 1 mL of Starscint and the mixture vortexed before scintillation counting. After background subtraction, the radiolabel content of the sample was corrected for the total volume of urine collected over that time interval and converted to a percentage of the total administered ^{3}H dose.

Feces were collected into preweighed vials and samples homogenized into a slurry by soaking in MilliQ water, prior to drying at 60 °C. Six replicate samples (20 mg) of the dried feces were then separated into two groups of $n = 3$ samples. One group of samples was processed without further addition, and one group of three samples was spiked with a known quantity of the radioactive dendrimer (approximately 500 dpm) to provide feces counting efficiency data (as above). The samples were then solubilized using the method described by Lyons et al..[32] Briefly, 2 mL of Soluene was added to remoistened feces and heated overnight at 60 °C. A further 2 mL of isopropyl alcohol was then added, and

the samples were heated for a further 2 h. The solubilized samples were then bleached with 400 μL of hydrogen peroxide (30% w/v) prior to the addition of 12 mL of Starscint. Samples were then left at room temperature for 4 days, prior to cooling at 4 °C for 24 h and subsequent scintillation counting at 12 °C. The total amount of ^{3}H excreted in feces was calculated using the total dry weight of feces collected. The LOQ for the assay was assumed to be 3 times the average counts in blank feces, since the mass of feces produced varied widely and therefore determination of a minimum quantifiable number of counts in a certain sample mass was not possible.

Size Exclusion Chromatography. Several methods were used to investigate the size of the species present in plasma samples. First, a coarse size separation was performed by eluting plasma samples through a PD10 gel filtration column (GE Healthcare, NSW, Australia) and collecting fractions under gravity. In this method, plasma samples (500 μL) were diluted with 2 mL of PBS prior to application to the top of a pre-equilibrated PD10 column. Fractions (500 μL) were collected manually into Eppendorf tubes, and 100 μL aliquots were added to 1 mL of Starscint prior to scintillation counting. Intact dendrimer and lysine solutions in PBS were also eluted through the column to characterize the retention volumes of the pure components.

To provide more information on the size of the radiolabel-containing species in plasma, an analytical size exclusion column (Superdex Peptide 10/300 GL, GE Healthcare, NSW, Australia) coupled to a Waters 590 HPLC pump (Millipore Corporation, Milford, MA) was subsequently used to generate more accurate separations. Plasma samples were again diluted in an equal volume of PBS and 100 μL of the mixture injected onto the column. Samples were eluted with PBS containing 0.3 M NaCl (pH 3.5) at 0.5 mL/min, and aliquots were collected at 1 min intervals using a Gilson FC10 fraction collector (John Morris Scientific Pty. Ltd., VIC, Australia). Aliquots were then mixed with Starscint (3 mL) and analyzed by liquid scintillation to determine the radioactivity in each fraction. Intact dendrimer and lysine solutions in PBS were again eluted separately through the column to characterize their retention volumes. Dendrimer and lysine were also incubated in fresh heparinized plasma for 1 h and the dendrimer−plasma or lysine−plasma mixtures analyzed by SEC. This analysis was performed to provide an indication of the possibility that physical interaction of dendrimer or lysine with plasma components may lead to the production of a high molecular weight species in plasma.

To obtain better resolution of the high molecular weight radiolabeled species present in plasma, samples were also analyzed using a Superdex 75 HR 10/30 size exclusion column (GE Healthcare, NSW, Australia). Aliquots (0.5 mL) were again collected at 1 min intervals, diluted in Starscint (3 mL), and analyzed by liquid scintillation counting to determine the radioactivity in each fraction. Protein standards were used to compose a standard curve (linear $R^2 = 0.9915$) which was used to estimate the molecular masses of the eluting proteins. Protein elution was monitored at 280 nm using a Waters 486 UV detector (Millipore Corporation, Milford, MA). The void volume of the column was determined using blue dextran 2000. Elution times for higher molecular weight proteins (molecular mass > 70 kDa) were obtained by injection of 20 μL of Precision Plus protein standard onto the column (Bio-Rad, Hercules, CA).

Pharmacokinetic Calculations. The concentrations of radiolabel in plasma/whole blood samples were converted to nanogram equivalent concentrations using the specific activity of the radiolabeled dendrimer. These concentrations have been expressed throughout this paper as nanogram equivalents/milliliter; however, this should be viewed with the caveat that this approach assumes that the ^{3}H radiolabel remains associated with the intact dendrimer, which as described below is not the case in some instances.

The rate of initial decline in the plasma concentration−time curves was estimated by linear regression of at least 3 points in the initial phase of the log−linear plasma concentration versus time plots. The rate constants obtained from these data have been described as "elimination" rate constants (K), but may not represent the true terminal elimination rate constants since the rapidity of elimination made accurate delineation of distribution and elimination events difficult. The half-life of this initial decline was estimated from $t_{1/2} = 0.693/K$. In all cases, an estimate of initial distribution volume (V_c) was calculated from the dose/$C_p°$, where $C_p°$ was the concentration in plasma at the moment of completion of the 2 min infusion. More detailed pharmacokinetic evaluation of the data, including identification of a true elimination rate constant and elimination half-life, was not possible due to the very rapid initial removal from plasma and unusual profiles at later time points.

Results

Synthesis and Characterization of Tritium-Labeled Cationic Dendrimers. The specific activity and molecular weight of the dendrimers (Scheme 1) are listed in Table 1. Detailed synthetic methods and HPLC, NMR, and MS characterization data of intermediates and products are reproduced in the Supporting Information.

Plasma Pharmacokinetics of Poly-L-lysine Dendrimers. The plasma concentration−time profiles for the uncapped, cationic dendrimers are shown in Figure 1. In the case of both BHALys $[Lys]_4$ $[^3H\text{-}Lys]_8$ $[NH_2]_{16}$ and BHALys $[Lys]_8$ $[^3H\text{-}Lys]_{16}$ $[NH_2]_{32}$ dendrimers, a very rapid initial drop in plasma concentration was evident, after which time (at approximately 30−60 min postdose) the concentration of radiolabel in the plasma increased, reaching a maximum at approximately 6−8 h postadministration.

Interestingly, after administration of the same dose, the initial plasma concentration of the smaller BHALys $[Lys]_4$ $[^3H\text{-}Lys]_8$ $[NH_2]_{16}$ dendrimer was approximately three times higher and the initial distribution volume (V_c) correspondingly three times smaller than that of the larger (i.e., higher molecular weight, generation 4) BHALys $[Lys]_8$ $[^3H\text{-}Lys]_{16}$ $[NH_2]_{32}$ dendrimer (Table 2, Figure 1).

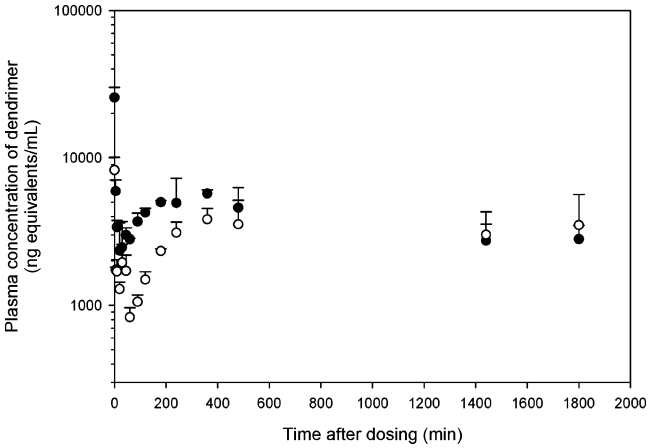

Figure 1. Plasma concentrations of cationic ^{3}H-dendrimers following intravenous administration at a dose of 5 mg/kg to rats (mean ± SD, $n = 3$). Closed symbols represent administration of BHALys $[Lys]_4$ $[^3H\text{-}Lys]_8$ $[NH_2]_{16}$, open symbols BHALys $[Lys]_8$ $[^3H\text{-}Lys]_{16}$ $[NH_2]_{32}$. The data are shown as ng equiv/mL of administered dendrimer.

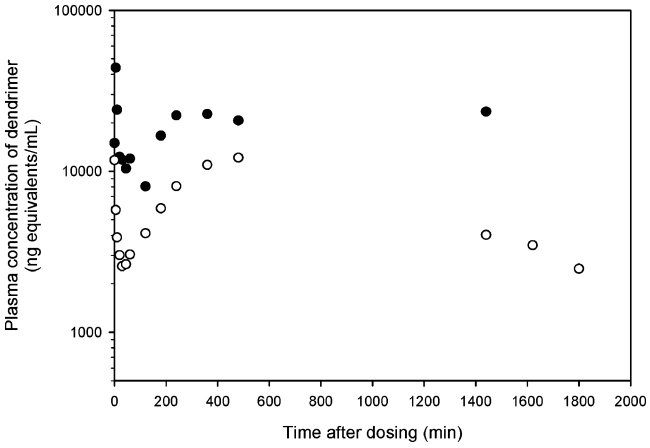

Figure 2. Plasma concentration of cationic ^{3}H-dendrimers following intravenous administration at higher doses in pilot studies to rats ($n = 1$). Closed symbols show data obtained after administration of 24.3 mg/kg BHALys $[Lys]_4$ $[^3H\text{-}Lys]_8$ $[NH_2]_{16}$, and open symbols represent data obtained after administration of 22.3 mg/kg BHALys $[Lys]_8$ $[^3H\text{-}Lys]_{16}$ $[NH_2]_{32}$. The data are shown as ng equiv/mL of administered dendrimer.

While the unusual behavior of the cationic dendrimers made it difficult to extract typical pharmacokinetic parameters such as clearance (Cl) and final distribution volumes (V_λ), the elimination of radiolabel from the plasma over the initial 10 min was approximately linear on a semilog plot, enabling calculation of an initial half-life which reflects the rate of initial decline in plasma radioactivity. The calculated initial plasma half-lives for BHALys $[Lys]_4$ $[^3H\text{-}Lys]_8$ $[NH_2]_{16}$ and BHALys $[Lys]_8$ $[^3H\text{-}Lys]_{16}$ $[NH_2]_{32}$ were 3.5 ± 0.2 min and 4.4 ± 0.4 min, respectively (Table 2).

Pilot ($n = 1$) studies of dendrimer pharmacokinetics at a dose approximately 5 times higher than that employed for the studies described above are presented in Figure 2 (redose was 24.3 and 22.6 mg/kg for BHALys $[Lys]_4$ $[^3H\text{-}Lys]_8$ $[NH_2]_{16}$ and BHALys $[Lys]_8$ $[^3H\text{-}Lys]_{16}$ $[NH_2]_{32}$, respectively). The plasma profiles showed qualitatively similar behavior to the 5 mg/kg dose. An initial rapid removal from plasma was again evident with an initial half-life of <10 min in both cases. A later rise in concentration was also apparent, reaching a maximum at 4−6 h. The pharmacokinetic behavior of the poly-L-lysine dendrimers was therefore not dramatically concentration dependent over the dose range of 5−25 mg/kg.

Whole Blood Pharmacokinetics of Poly-L-lysine Dendrimers. Qualitatively, the whole blood concentration−time profiles (Figure 3) were similar to the plasma profiles, suggesting that the unusual plasma pharmacokinetics profiles were also not influenced by, or a result of, blood partitioning. Quantitatively, the whole blood concentrations of BHALys $[Lys]_4$ $[^3H\text{-}Lys]_8$ $[NH_2]_{16}$ were generally lower than the

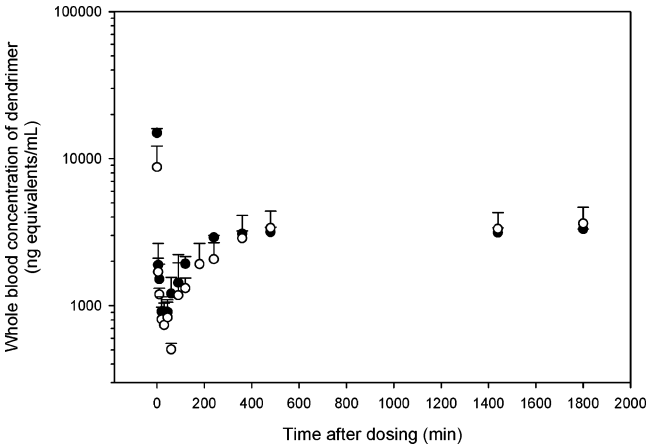

Figure 3. Whole blood concentrations of cationic ^{3}H-dendrimers following intravenous administration at a dose of 5 mg/kg to rats (mean ± SD, $n = 3$). Closed symbols represent administration of BHALys $[Lys]_4$ $[^3H\text{-}Lys]_8$ $[NH_2]_{16}$, open symbols BHALys $[Lys]_8$ $[^3H\text{-}Lys]_{16}$ $[NH_2]_{32}$. The data are shown as ng equiv/mL of administered dendrimer.

Table 2. Plasma Pharmacokinetic Parameters after Intravenous Administration of ^{3}H-Dendrimers at 5 mg/kg (Mean ± SD, $n = 3$)

dendrimer	$C_p°$ (μg/mL)	initial k (h^{-1})	initial $t_{1/2}$ (min^{-1})	V_c (mL)
		Plasma		
BHALys $[Lys]_4$ $[^3H\text{-}Lys]_8$ $[NH_2]_{16}$	24.7 ± 6.5	12.1 ± 1.0	3.5 ± 0.2	55.9 ± 11.8
BHALys $[Lys]_8$ $[^3H\text{-}Lys]_{16}$ $[NH_2]_{32}$	8.4 ± 2.2	9.5 ± 0.1	4.4 ± 0.4	163 ± 34.6
BHALys $[Lys]_4$ $[^3H\text{-}Lys]_8$ $[D\text{-}Lys]_{16}$ $[NH_2]_{32}$	12.4 ± 1.1	14.4 ± 0.5	3.0 ± 0.0	99.4 ± 10.1
		Whole Blood		
BHALys $[Lys]_4$ $[^3H\text{-}Lys]_8$ $[NH_2]_{16}$	15.0 ± 1.1	13.9 ± 2.1	3.0 ± 0.5	96.1 ± 13.2
BHALys $[Lys]_8$ $[^3H\text{-}Lys]_{16}$ $[NH_2]_{32}$	8.8 ± 3.4	11.7 ± 2.5	3.7 ± 0.7	190.4 ± 82.2

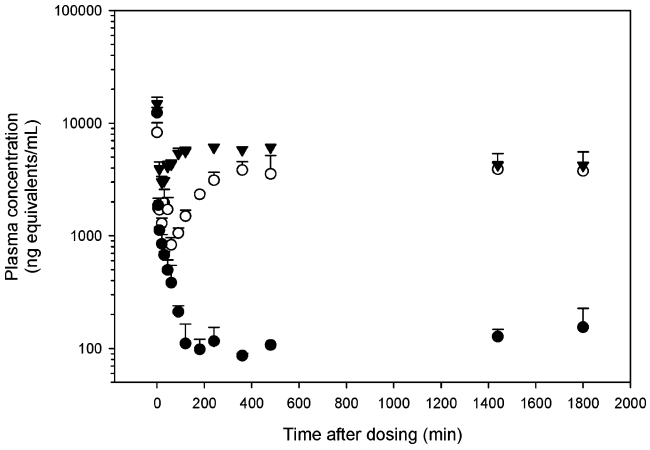

Figure 4. Plasma concentrations of BHALys $[Lys]_8$ $[^3H\text{-}Lys]_{16}$ $[NH_2]_{32}$, BHALys $[Lys]_4$ $[^3H\text{-}Lys]_8$ $[D\text{-}Lys]_{16}$ $[NH_2]_{32}$, and L-lysine following intravenous administration at 5 mg/kg to rats (mean ± SD, $n = 3$). Open circles represent administration of BHALys $[Lys]_8$ $[^3H\text{-}Lys]_{16}$ $[NH_2]_{32}$, closed circles BHALys $[Lys]_4$ $[^3H\text{-}Lys]_8$ $[D\text{-}Lys]_{16}$ $[NH_2]_{32}$, and closed triangles L-lysine. The data are shown as ng equiv/mL of administered dendrimer or lysine.

plasma concentrations by a factor of approximately 2 (Figure 1), suggesting that the smaller dendrimer was effectively excluded from the red cell fraction of whole blood in vivo. In contrast, the blood and plasma pharmacokinetic profiles of the higher molecular weight (and more highly charged) BHALys $[Lys]_8$ $[^3H\text{-}Lys]_{16}$ $[NH_2]_{32}$ dendrimer were more similar, suggesting a greater capacity for the more highly charged dendrimer to interact with red blood cells.

Plasma Pharmacokinetics of a Poly-L-lysine Based Dendrimer with a D-Lysine Surface. The unusual pharmacokinetic behavior exhibited by the poly-L-lysine dendrimers was thought to result from rapid binding of the intact dendrimer to the vasculature (leading to very rapid removal from the circulating plasma), followed by enzymatic breakdown of the poly-amino acid structure and release of free ^3H-labeled lysine back into the plasma at later time points. To examine this hypothesis, BHALys $[Lys]_4$ $[^3H\text{-}Lys]_8$ $[D\text{-}Lys]_{16}$ $[NH_2]_{32}$ was administered identically to its all-L-lysine counterpart BHALys $[Lys]_8$ $[^3H\text{-}Lys]_{16}$ $[NH_2]_{32}$ on the assumption that covering the dendrimer surface with "non-natural" D-lysine would likely block the action of proteases on the dendrimer but not interfere with other binding and clearance processes. To facilitate evaluation of the pharmacokinetics of the D-lysine dendrimer at later time points where plasma levels were expected to be low, the radiolabeled core material subsequently capped with D-Lys was synthesized to specific activity higher than that of the L-Lys capped material. In all other respects, however, the core materials were identical.

The plasma pharmacokinetics of BHALys $[Lys]_4$ $[^3H\text{-}Lys]_8$ $[D\text{-}Lys]_{16}$ $[NH_2]_{32}$ are shown in Figure 4. BHALys $[Lys]_4$ $[^3H\text{-}Lys]_8$ $[D\text{-}Lys]_{16}$ $[NH_2]_{32}$ was rapidly removed from plasma similarly to the corresponding all-L-lysine dendrimer with an initial plasma half-life of 3 min (Table 2). BHALys $[Lys]_4$ $[^3H\text{-}Lys]_8$ $[D\text{-}Lys]_{16}$ $[NH_2]_{32}$ also had comparable initial plasma concentrations and immediate distribution volumes (Table 2). Importantly, however, a secondary maximum in the plasma concentration time profiles was not seen. Instead, the plasma concentrations of the D-lysine dendrimer continued to decline over 4 h following the iv dose, suggesting that metabolism had been significantly inhibited. At later times the decline in the plasma concentration−time profile slowed and plasma concentrations plateaued, potentially reflecting delayed bioprocessing.

To further interrogate the possibility that enzymatic cleavage of the poly-L-lysine dendrimer may be responsible for the secondary maxima, we also investigated the plasma pharmacokinetics of monomeric ^3H-L-lysine following iv administration. These studies were conducted on the premise that, if the re-entry of ^3H into the circulation was due to incorporation of ^3H-labeled monomeric lysine into protein resynthesis pathways, then the pharmacokinetic profiles of monomeric and dendritic L-lysine should be similar at least at later time points. Figure 4 illustrates the pharmacokinetic profile following iv administration of ^3H-L-lysine. Similarly to BHALys $[Lys]_8$ $[^3H\text{-}Lys]_{16}$ $[NH_2]_{32}$, the plasma concentration of monomeric lysine declined rapidly over the first 30 min period postdose followed by a secondary increase in plasma ^3H levels which reached a maximum approximately 3 h after administration.

Speciation of Radiolabel in Plasma Samples. In order to better describe the ultimate fate of the ^3H initially administered as the poly-L-lysine dendrimer, size exclusion chromatography (SEC) was employed to further investigate the nature of the ^3H label present in the plasma at 6−8 h after iv administration of the BHALys $[Lys]_8$ $[^3H\text{-}Lys]_{16}$ $[NH_2]_{32}$ dendrimer.

SEC separation of the 6 h plasma sample obtained after administration of BHALys $[Lys]_8$ $[^3H\text{-}Lys]_{16}$ $[NH_2]_{32}$ using a PD10 desalting column showed that the radiolabel eluted at two different elution volumes (approximately 4 mL and 8 mL), suggesting the presence of two different radiolabeled species in plasma (data not shown). In control experiments, where dendrimer and lysine dissolved in PBS were applied to the column, the dendrimer eluted in the void volume of the column (elution volume 4 mL), while lysine eluted at an elution volume of approximately 8 mL. This preliminary separation suggested that total radiolabel in the plasma at 6 h was present as both (1) a large species of size equal to or greater than that of the dendrimer and (2) a proportion of free ^3H-lysine. This finding prompted further attempts to better define the ^3H-containing species in plasma using conventional size exclusion chromatography.

A Superdex Peptide column was initially employed to provide improved separation of the high molecular weight radiolabeled material present in plasma. Using this column, the elution times of lysine and dendrimer were 42 and 21 min, respectively (Figure 5). To eliminate the possibility of physical binding of labeled dendrimer and/or labeled lysine fragments to plasma proteins being responsible for the larger ^3H-containing species, control experiments were performed

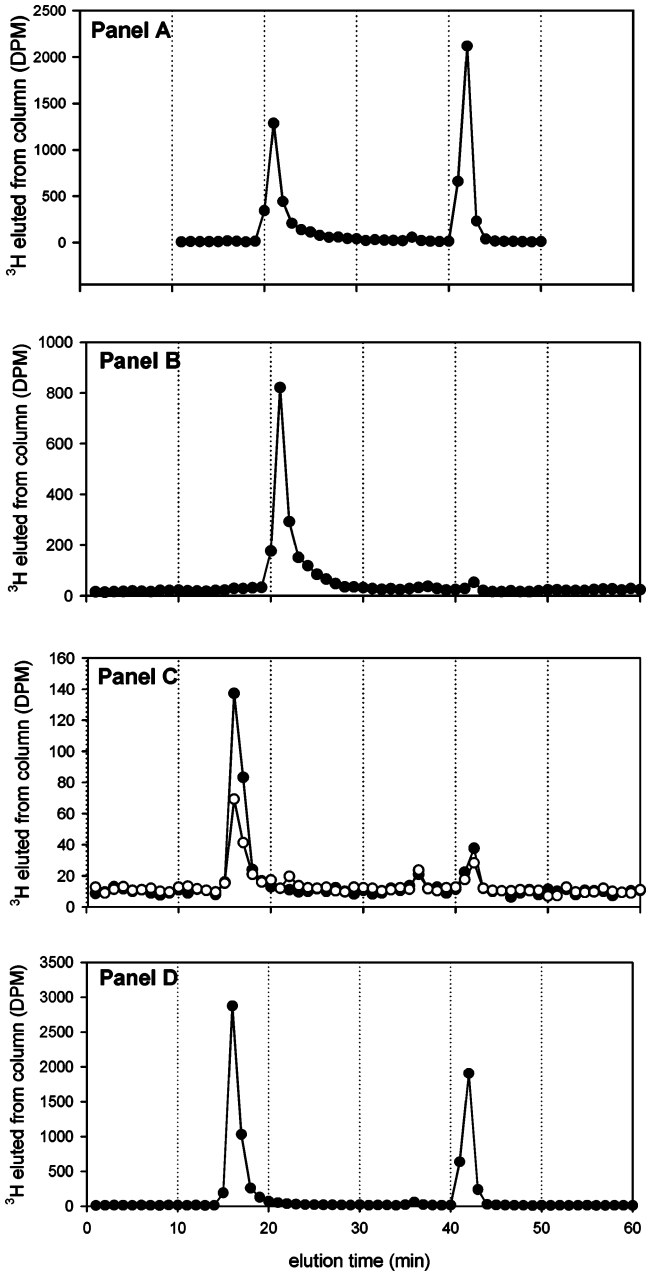

Figure 5. Size exclusion chromatography (SEC) profiles obtained using a Superdex Peptide 10/300 GL size exclusion column. Panel A: BHALys $[Lys]_8$ $[^3H\text{-}Lys]_{16}$ $[NH_2]_{32}$ ($t_R = 21$ min) and lysine ($t_R = 42$ min) after incubation in heparinized blank plasma for 1 h at room temperature. The elution volumes and profiles were identical to those obtained for BHALys $[Lys]_8$ $[^3H\text{-}Lys]_{16}$ $[NH_2]_{32}$ and lysine (profile not shown). Panel B: Plasma sample taken immediately ($t = 0$) after intravenous administration of BHALys $[Lys]_8$ $[3H\text{-}Lys]_{16}$ $[NH_2]_{32}$. Panel C: Plasma samples taken 3 h (open symbols) and 6 h (closed symbols) after intravenous administration of BHALys $[Lys]_8$ $[^3H\text{-}Lys]_{16}$ $[NH_2]_{32}$. Panel D: Plasma sample taken 30 h after intravenous administration of L-lysine. The peak at 16 min represents a high molecular weight species eluting at the void volume of the column.

in which the dendrimer and free lysine were incubated for 1 h with fresh heparinized plasma before elution through the column. Panel A in Figure 5 shows that incubation of ^{3}H-dendrimer and ^{3}H-lysine with plasma had no effect on the retention time (t_R) of either component when compared to the retention times of the same material after dissolving in PBS, suggesting that physical binding of the dendrimer or lysine to plasma components did not occur, or that the components were separated during SEC.

Plasma samples taken at different times after administration of ^{3}H-BHALys $[Lys]_8$ $[^3H\text{-}Lys]_{16}$ $[NH_2]_{32}$ were then analyzed by SEC to investigate the disposition of the ^{3}H label over time. Elution of a sample taken at $t = 0$ min, i.e., immediately after the completion of the iv infusion (Figure 5, panel B), produced a single primary peak which eluted at a retention time coincident with that of intact dendrimer (16 min). A very minor peak was also observed at the retention time of lysine (42 min).

Elution of a plasma sample obtained 3 h after administration of BHALys $[Lys]_8$ $[^3H\text{-}Lys]_{16}$ $[NH_2]_{32}$ (Figure 5, panel C) resulted in two principal peaks, one smaller peak at the retention time of lysine, and a second and larger peak at 16 min, coincident with the exclusion volume of the Superdex Peptide column. This suggested that the ^{3}H eluting at this volume was associated with a high molecular weight species (molecular mass > 20 kDa), which was considerably larger than parent dendrimer. A small peak was also evident at 21 min, likely reflecting a small quantity of residual dendrimer in plasma, and a fourth minor peak was also evident at 36 min. This peak was not analyzed further, but the apparent molecular weight is consistent with that of saccharopine (a metabolite of lysine with approximately twice the MW of the parent amino acid) or a lysine dimer.

When the plasma sample obtained 6 h after administration of BHALys $[Lys]_8$ $[^3H\text{-}Lys]_{16}$ $[NH_2]_{32}$ was analyzed (Figure 5, panel C), an SEC pattern similar to that seen with the 3 h postdose sample was evident, although the size of the peak eluting at 16 min was increased.

To provide further evidence of the nature of the peak eluting at 16 min after SEC of the 3 and 6 h plasma samples obtained after administration of BHALys $[Lys]_8$ $[^3H\text{-}Lys]_{16}$ $[NH_2]_{32}$, a 30 h plasma sample taken from a rat administered monomeric L-lysine (i.e., the 30 h plasma sample from the L-lysine pharmacokinetic data described in Figure 5) was also analyzed by SEC (Figure 5, panel D). While a peak corresponding to the elution time of free lysine was present at 42 min, a large peak, which eluted at an elution time coincident with that of the high molecular weight species (16 min) seen in the profiles obtained from the BHALys $[Lys]_8$ $[^3H\text{-}Lys]_{16}$ $[NH_2]_{32}$ plasma samples, was also evident.

In an attempt to obtain better resolution of the high molecular weight species (i.e., the species which eluted at approximately 16 min after application to the Superdex Peptide column), a plasma sample obtained 6 h after administration of BHALys $[Lys]_8$ $[^3H\text{-}Lys]_{16}$ $[NH_2]_{32}$ and a plasma sample obtained 30 h after administration of L-lysine were also analyzed by SEC using a Superdex 75 column. The Superdex 75 column allows resolution of molecular weights ranging from 3000 and 70 000 and was utilized to

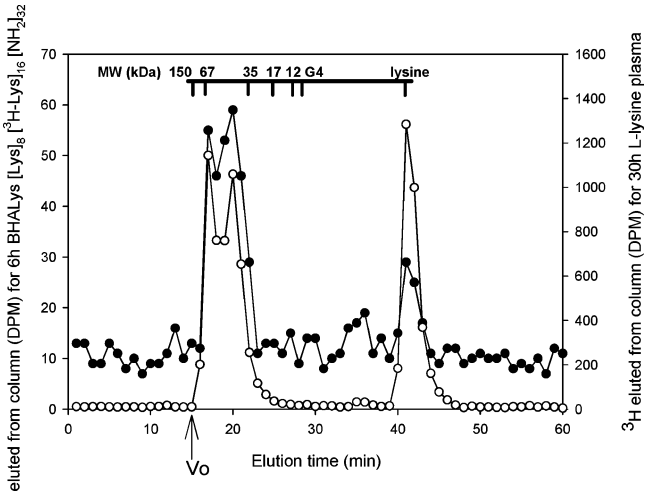

Figure 6. Elution profiles of plasma radiolabel (as eluted dpm) from a Superdex 75 HR 10/30 size exclusion column. Closed symbols represent the elution profile for a plasma sample taken 6 h after intravenous administration of BHALys $[Lys]_8$ $[^3H\text{-}Lys]_{16}$ $[NH_2]_{32}$ (scale on left-hand *Y* axis). Open symbols represent the elution profile for a plasma sample taken 30 h after intravenous infusion of L-lysine (scale on right-hand *Y* axis). The elution times for various MW protein standards, BHALys $[Lys]_8$ $[^3H\text{-}Lys]_{16}$ $[NH_2]_{32}$ (G4), and lysine are shown at the top of the graph. The void volume of the column was determined by injection of blue dextran 2000 (molecular mass 2000 kDa) and is indicated below the figure (Vo).

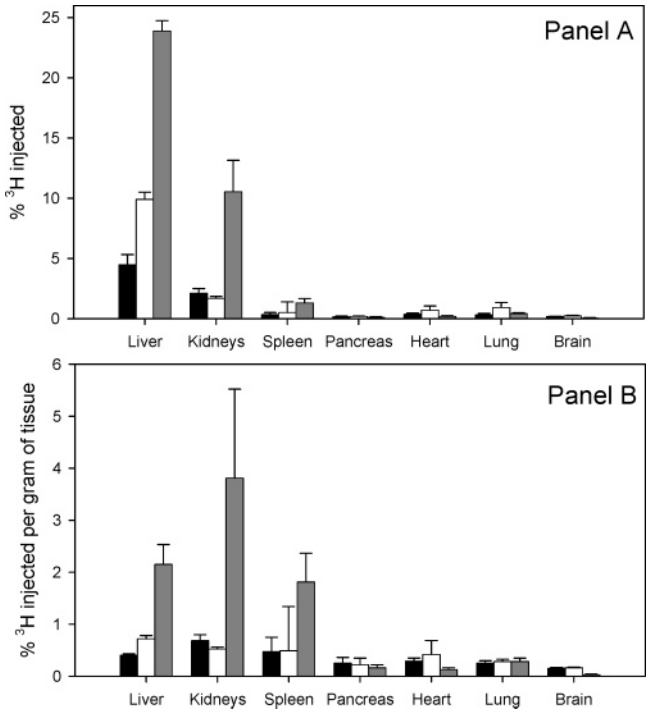

Figure 7. Distribution of residual ^3H in major organs at 30 h after intravenous administration of cationic ^3H-dendrimers at 5 mg/kg to rats. Panel A is data presented as % of injected radiolabel, while for panel B the data is presented as % of injected radiolabel per gram of tissue (mean ± SD, $n = 3$). Closed symbols represent the tissue biodistribution for BHALys $[Lys]_4$ $[^3H\text{-}Lys]_8$ $[NH_2]_{16}$, while open symbols represent the tissue biodistribution for BHALys $[Lys]_8$ $[^3H\text{-}Lys]_{16}$ $[NH_2]_{32}$. Shaded (gray) symbols represent the tissue biodistribution for BHALys $[Lys]_4$ $[^3H\text{-}Lys]_8$ $[D\text{-}Lys]_{16}$ $[NH_2]_{32}$.

improve resolution at higher molecular weights. As shown in Figure 6, the SEC profiles of the plasma samples obtained after administration of both intact dendrimer and free lysine were again qualitatively similar, suggesting the presence of the same species in the plasma in both cases. The Superdex 75 column, however, allowed better resolution of the large molecular weight species which resolved into two broad peaks with retention times corresponding approximately to the molecular weights of globular proteins of 67 000 and 55 000. Lysine was again present at an elution time of 42 min in both profiles.

Excretion of Dendrimers in Urine and Feces. The results for the excretion of radiolabel in the urine and feces are presented in Table 3. The cationic dendrimers were not substantially renally cleared as evidenced by recovery of <10% of the administered radiolabel dose in the urine over the sampling period. The levels of radioactivity in pooled feces were below the nominal LOQ of the assay.

Biodistribution of Radiolabel in Major Organs 30 h after Dosing. The biodistribution data for the three cationic poly-L-lysine dendrimers is shown in Figure 7. The data in panel A, expressed as a percentage of the total radiolabel dosed, reveal that the majority of the ^3H recovered in the organs 30 h after administration of both the poly-L-lysine dendrimers was present in the liver and kidneys. The level of radiolabel present in the liver 30 h after dosing BHALys $[Lys]_4$ $[^3H\text{-}Lys]_8$ $[NH_2]_{16}$ (4.5 ± 0.8%) was approximately half of that after dosing BHALys $[Lys]_8$ $[^3H\text{-}Lys]_{16}$ $[NH_2]_{32}$ (9.9 ± 0.6%) ($p < 0.001$). When the distribution data were expressed per gram of tissue (panel B), however, a relatively even distribution between the different organs was apparent, suggesting little preferential organ accumulation.

The biodistribution data for the D-Lys dendrimer revealed more specific organ distribution patterns. Figure 7, panel A, shows that the majority of ^3H recovered in the organs 30 h

Table 3. Excretion of ^3H over 30 h from Rats after Intravenous Administration of Cationic ^3H-Dendrimers at 5 mg/kg (Mean ± SD, $n = 3$)

	recovery (% of injected dose)	
dendrimer	in urine	in feces
BHALys $[Lys]_4$ $[^3H\text{-}Lys]_8$ $[NH_2]_{16}$	7.5 ± 1.3	below LOQ (LOQ = 1.6%)
BHALys $[Lys]_8$ $[^3H\text{-}Lys]_{16}$ $[NH_2]_{32}$	4.0 ± 0.2	below LOQ (LOQ = 0.7%)
BHALys $[Lys]_4$ $[^3H\text{-}Lys]_8$ $[D\text{-}Lys]_{16}$ $[NH_2]_{32}$	3.9 ± 0.9	below LOQ (LOQ = 1.2%)

after BHALys $[Lys]_4$ $[^3H\text{-}Lys]_8$ $[D\text{-}Lys]_{16}$ $[NH_2]_{32}$ dosing was located in the liver and kidneys. Recovery of ^3H in the liver and kidneys from BHALys $[Lys]_4$ $[^3H\text{-}Lys]_8$ $[D\text{-}Lys]_{16}$ $[NH_2]_{32}$ dosed rats was approximately 2.5× and 7× higher than in the respective organs from BHALys $[Lys]_8$ $[^3H\text{-}Lys]_{16}$ $[NH_2]_{32}$ dosed rats. When the organ biodistribution data was normalized for tissue mass (panel B), accumulation of ^3H in the liver, kidneys, and spleen was also apparent.

Discussion

The potential utility of dendritic polymers both as drug delivery vectors and as pharmaceutical actives has received increasing interest in recent years.[2,33] However, while the literature is replete with reports of, for example, synthetic schemes for dendrimer assembly, descriptions of dendrimer−drug interactions and drug loading efficiencies, and, increasingly, in vitro evaluations of dendrimer interactions with cell lines,[8,11,17,34] there is very little information describing the fundamental pharmacokinetic and metabolic fate of dendrimers. The studies described in the current communication were designed to address this gap in the literature and specifically to evaluate the pharmacokinetics of 3rd and 4th generation poly-L-lysine dendrimers (BHALys $[Lys]_4$ $[^3H\text{-}Lys]_8$ $[NH_2]_{16}$ and BHALys $[Lys]_8$ $[^3H\text{-}Lys]_{16}$ $[NH_2]_{32}$, respectively) after intravenous administration to rats. Since there is considerable interest in the metabolic fate of potential drug candidates or drug delivery vectors, the present study also examined in some detail the potential for biodegradation and bioresorption of poly-L-lysine dendrimers.

After intravenous administration, both BHALys $[Lys]_4$ $[^3H\text{-}Lys]_8$ $[NH_2]_{16}$ and BHALys $[Lys]_8$ $[^3H\text{-}Lys]_{16}$ $[NH_2]_{32}$ were very rapidly removed from plasma, exhibiting initial plasma half-lives of less than 10 min (Figure 1, Table 2). This initial rapid loss was not markedly dependent on dose (Figure 2), and was also evident when whole blood (as opposed to plasma) profiles were examined (Figure 3), and when the L-lysine surface groups were changed to D-lysine (Figure 4). Interestingly, the initial distribution volumes (V_c) were surprisingly high for these relatively high molecular weight species, and the V_c of the higher molecular weight generation 4 dendrimers BHALys $[Lys]_8$ $[^3H\text{-}Lys]_{16}$ $[NH_2]_{32}$ and BHALys $[Lys]_4$ $[^3H\text{-}Lys]_8$ $[D\text{-}Lys]_{16}$ $[NH_2]_{32}$ were higher than the V_c of the smaller generation 3 comparator. The V_c values for the 3rd and 4th generation dendrimers appear, therefore, to be more highly correlated with surface charge, rather than molecular weight. The data are consistent with the initial "distribution" process reflecting rapid binding of the polycationic dendrimers to the vascular endothelium, in a process driven by electrostatic interactions, leading to loss from the circulating plasma. In contrast, typical extravasation processes seem unlikely since rapid passage across the vascular endothelium would be difficult for such highly charged macromolecules, and would be expected to increase with reductions in molecular weight and surface charge, whereas the opposite was in fact observed. These trends were also evident in the whole blood pharmacokinetics, although in the case of the smaller dendrimer the $C_p°$ values were approximately 2-fold lower (and the corresponding V_c values 2-fold higher), suggesting that binding of the dendrimers to red blood cells was lower for the less highly charged generation 3 dendrimers.

The rapid removal of the poly-L-lysine dendrimers from the plasma and the potential role of binding to the vasculature in this process are consistent with previous studies. For example, Johnston et al.[35] reported an elimination half-life of 1.49 min following intravenous administration of FITC-labeled poly-L-lysine to rats, and poly-L-lysine:DNA complexes have also been shown to be cleared from circulation with a $t_{1/2}$ of less than 5 min.[36] Cationic PAMAM dendrimers are also rapidly cleared from the circulation, with only approximately 1% of an injected dose of generation 3 and 4 PAMAM dendrimers remaining in the blood 1 h postdose. Interestingly, in the same study, approximately 20% of the corresponding anionic PAMAM dendrimer (which displays a carboxylate surface) remained in the circulation at the same time point.[18] Wilbur et al.[37] have also shown that less than 0.5% of the injected dose of a biotin-conjugated PAMAM dendrimer remains in the blood 4 h after intravenous injection. PAMAM dendrimers (generations 3−6) derivatized with large chelating ligands to facilitate complexation of gadolinium ions for imaging applications have also been shown to be cleared rapidly from the circulation at early times, with blood half-lives of less than 10 min, although later elimination half-lives were closer to 1 h.[38]

The suggestion that binding to endothelial surfaces is a key process in the clearance of cationic poly-L-lysine dendrimers is further supported by the recent studies of

(33) McCarthy, T. D.; Karellas, P.; Henderson, S. A., Giannis, M.; O'Keefe, D. F.; Heery, G.; Paull, J. R. A.; Matthews, B. R.; Holan, G. Dendrimers as Drugs: Discovery and Preclinical and Clinical Development of Dendrimer-Based Microbicides for HIV and STI Prevention. *Mol. Pharm.* **2005**, *2*, 312−318.

(34) Stevelmans, S.; van Hest, J. C. M.; Jansen, J. F. G. A.; van Boxtel, D. A. F. J.; de Brabander-van den Berg, E. M. M.; Meijer, E. W. Synthesis, Characterization, and Guest−Host Properties of Inverted Unimolecular Dendritic Micelles. *J. Am. Chem. Soc.* **1996**, *118*, 7398−7399.

(35) Johnston, T. P.; Kuchimanchi, K. R.; Alur, H.; Chittchang, M.; Mitra, A. K. Inducing a Change in the Pharmacokinetics and Biodistribution of Poly-L-Lysine in Rats by Complexation with Heparin. *J. Pharm. Pharmacol.* **2003**, *55*, 1083−1090.

(36) Dash, P. R.; Read, M. L.; Barrett, L. B.; Wolfert, M. A.; Seymour, L. W. Factors Affecting Blood Clearance and In Vivo Distribution of Polyelectrolyte Complexes for Gene Delivery. *Gene Ther.* **1999**, *6*, 643−650.

(37) Wilbur, D. S.; Pathare, P. M.; Hamlin, D. K.; Buhler, K. R.; Vessella, R. L. Biotin Reagents for Antibody Pretargeting. 3. Synthesis, Radioiodination, and Evaluation of Biotinylated Starburst Dendrimers. *Bioconjugate Chem.* **1998**, *9*, 813−825.

(38) Kobayashi, H.; Sato, N.; Hiraga, A.; Saga, T.; Nakamoto, Y.; Ueda, H.; Konishi, J.; Togashi, K.; Brechbiel, M. W. 3D-Micro-MR Angiography of Mice Using Macromolecular MR Contrast Agents with Polyamidoamine Dendrimer Core with Reference to Their Pharmacokinetic Properties. *Magn. Reson. Med.* **2001**, *45*, 454−460.

Sakharov et al.[39] in which a number of molecules with potential vascular binding properties were investigated with a view to their use as drug delivery vehicles to the vascular lumen. In these studies, both linear poly-L-lysine and PAMAM dendrimers were found to bind strongly to the vascular endothelium. The strength of the endothelial binding also increased with increasing molecular weight, consistent with the higher V_c data in the current study for the higher molecular weight BHALys $[Lys]_8$ $[^3H\text{-}Lys]_{16}$ $[NH_2]_{32}$ dendrimer.

A notable difference between this and other studies of dendrimer pharmacokinetics is the apparent reappearance of radiolabel in both plasma and blood at later time points. One explanation for this data is that, after an initial rapid removal from plasma (mediated most likely via binding to endothelial cell surfaces), poly-L-lysine dendrimers are subsequently subject to enzymatic breakdown liberating free lysine that is in turn incorporated into protein biosynthetic pathways.

In support of this hypothesis, both linear and branched poly-L-lysine are rapidly degraded in the presence of exopeptidase aminopeptidase M or endopeptidase trypsin,[40] and therefore proteolysis of dendritic poly-L-lysine seems likely. While previous studies have detailed the pharmacokinetics of linear poly-L-lysine after intravenous injection[35] and have not described a subsequent reincorporation into protein biosynthetic pathways, this most likely reflects the time scales under which these previous studies were conducted (10 min) rather than any significant differences between the susceptibility of dendritic, as opposed to linear, poly-L-lysine, to enzymatic attack. Interestingly, in the current studies when an equivalent sized dendrimer, but one which presented a D-lysine surface, was administered, a similar rapid loss of dendrimer from plasma occurred over the first 10 min postdose, but little evidence of subsequent reappearance of radiolabel into the plasma was seen at earlier times. This suggests that substitution of the L-lysine surface groups with D-lysine did not alter the initial process of dendrimer binding to the endothelium (which would be expected since the overall net charge was unaltered) but that proteolytic breakdown was greatly inhibited by the coverage in "non-natural" D amino acids.

The SEC data provides further evidence of the liberation of free lysine from the cationic dendrimers, and radiolabeled species with apparent molecular weights consistent with that of lysine were seen in plasma samples obtained from animals administered the BHALys $[Lys]_8$ $[^3H\text{-}Lys]_{16}$ $[NH_2]_{32}$ dendrimer. A second, high molecular weight species was also evident in the plasma after administration of the poly-L-lysine dendrimer, consistent with the reincorporation of lysine into protein biosynthetic pathways. While only the BHALys $[Lys]_8$ $[^3H\text{-}Lys]_{16}$ $[NH_2]_{32}$ dendrimer was examined by size exclusion chromatography, the similar plasma concentration−time profiles for the Lys_8 dendrimer suggest that it is likely that the same processes occurred for both dendrimers. Incubation of both ^3H dendrimer and lysine with plasma and subsequent analysis suggested that this high molecular weight species did not result from simple association of the labeled dendrimer or lysine with endogenous components in the plasma leading to chromatographic separation of an apparently high molecular weight material. The high molecular weight species was also not present in the plasma of animals immediately after injection of dendrimer (i.e., $t = 0$), suggesting that its production was not rapid, a situation seemingly inconsistent with a simple association of label with endogenous macromolecules (or the presence of a contaminant in the injected material). It is more likely therefore that the high molecular weight species resulted from incorporation of ^3H lysine (liberated by enzymatic breakdown of the poly-L-lysine dendrimer), into normal biosynthetic pathways. The suggestion that the high molecular weight material is derived from lysine is also consistent with the similarity in SEC profiles of plasma samples taken from animals administered either BHALys $[Lys]_8$ $[^3H\text{-}Lys]_{16}$ $[NH_2]_{32}$ dendrimer or ^3H lysine.

Determination of the exact nature of the high molecular weight materials observed here by SEC was beyond the scope of the current study. The profiles presented, however, are consistent with the suggestion that lysine, liberated from the dendrimer by biodegradation, is reincorporated into protein biosynthetic pathways leading to the presence of a range of radiolabeled proteins in plasma. Subsequent studies will address the nature of the reincorporation products in more detail.

While there are relatively few studies investigating the pharmacokinetic behavior of dendrimers, there are a larger number of publications that report biodistribution data. For example, Kobayashi and colleagues have demonstrated the potential to tailor the properties of dendrimers to achieve selective targeting of dendrimer−gadolinium complexes to specific organs for imaging applications. In particular, positively charged dendrimers were found to accumulate preferentially in the liver and kidney, when compared with their negatively charged equivalents.[18,41,42] In contrast, in the current studies, the removal of poly-L-lysine dendrimers from the plasma was not associated with significant accumulation

(39) Sakharov, D. V.; Jie, A. F.; Bekkers, M. E.; Emeis, J. J.; Rijken, D. C. Polylysine as a Vehicle for Extracellular Matrix-Targeted Local Drug Delivery, Providing High Accumulation and Long-Term Retention Within the Vascular Wall. *Arterioscler., Thromb., Vasc. Biol.* **2001**, *21*, 943−948.

(40) Hudecz, F.; Kutassi-Kovacs, S.; Mezo, G.; Szekerke, M. Biodegradability of Synthetic Branched Polypeptide with Poly(L-lysine) Backbone. *Biol. Chem. Hoppe-Seyler* **1989**, *370*, 1019−1026.

(41) Kobayashi, H.; Sato, N.; Kawamoto, S.; Saga, T.; Hiraga, A.; Haque, T. L.; Ishimori, T.; Konishi, J.; Togashi, K.; Brechbiel, M. W. Comparison of the Macromolecular MR Contrast Agents with Ethylenediamine-Core Versus Ammonia-Core Generation-6 Polyamidoamine Dendrimer. *Bioconjugate Chem.* **2001**, *12*, 100−107.

(42) Sato, N.; Park, C. W.; Kim, H. S.; Han, E. S.; Wong, K. J.; Paik, R. S.; Park, L. S.; Yao, Z. S.; Carrasquillo, J. A.; Paik, C. H. Synthesis of Dendrimer-Based Biotin Radiopharmaceuticals to Enhance Whole-Body Clearance. *Nucl. Med. Biol.* **2003**, *30*, 617−625.

in either the kidney or the organs of the reticuloendothelial system, although the relatively large organ weight of the liver led to a larger absolute recovery of radiolabel in this organ. The amount of ^{3}H recovered in the liver after administration of BHALys $[Lys]_8$ $[^3H\text{-}Lys]_{16}$ $[NH_2]_{32}$ was approximately twice that recovered after administration of BHALys $[Lys]_4$ $[^3H\text{-}Lys]_8$ $[NH_2]_{16}$, most likely reflecting both the larger size and greater surface charge density of the larger dendrimer. When the current uptake data were normalized for organ mass, however, it is clear that the extent of accumulation in the organs examined was low and relatively nonspecific, and may reflect both the nonspecific redistribution of resynthesized protein in addition to the initial deposition patterns of intact dendrimer. In contrast, the D-lysine capped dendrimer, which does not undergo the same metabolic degradation as the all-L-lysine dendrimers, provided distribution patterns that were more targeted toward the organs of the reticuloendothelial system, namely, the liver and spleen, with a significant proportion of radiolabel also recovered in the kidneys.

Conclusions

The current data have shown that uncapped poly-L-lysine dendrimers are rapidly removed from the plasma on intravenous injection and that, at later time points, radiolabel initially associated with intact dendrimer reappears in the plasma associated with species that coelute on SEC with free lysine and a number of larger molecular weight (possibly proteinaceous) materials. The data also suggest that the highly charged cationic dendrimers rapidly bind to endothelial cell surfaces immediately after injection and are subsequently hydrolyzed to produce circulating free lysine, which is itself likely reincorporated into protein biosynthetic pathways. These data are, to our knowledge, the first to describe the in vivo biodegradation and resorption of poly-L-lysine dendrimers. The data further suggest that appropriate manipulation of the surface properties of poly-L-lysine dendrimers to enhance initial residence time in the plasma, but that eventually reveals the uncapped poly-L-lysine surface, may lead to the development of biodegradable and bioresorbable dendrimer-based drug delivery systems.

Acknowledgment. This work was funded by an Australian Research Council Linkage grant.

Supporting Information Available: Detailed descriptions of synthetic procedures for the dendrimers described here and supporting mass spectra. This material is available free of charge via the Internet at http://pubs.acs.org.

MP060032E